Network Formation and Sieving Performance of Self-Assembling Hydrogels

Rob G. H. Lammertink and Julia A. Kornfield*

Division of Chemistry and Chemical Engineering, 210-41 California Institute of Technology, Pasadena, California 91125

Received November 12, 2002; Revised Manuscript Received August 5, 2003

ABSTRACT: Self-assembling hydrogels, consisting of aqueous solutions of poly(ethylene glycol)s end-capped with perfluorocarbon groups (R_f−PEGs), were studied for their electrophoretic sieving performance. These materials form physical gels, with the end groups aggregated in hydrophobic cores. The gels display high sieving performance, expressed as a large mobility dependence on DNA size, for short double-stranded DNA fragments even at relatively low polymer concentrations (∼3 wt %). This interesting characteristic can be attributed to the dense packing of interconnected micelles that build up the hydrogel network. The physically connected micelles act as a permanent network on the time scale of DNA migration over the distance between micelle cores. A mobility plateau was observed for intermediate DNA sizes that were probably too large to sieve through the network of interconnected micelles and yet too small to reptate. This plateau was followed by a reptation regime for larger DNA sizes, that has similar resolving characteristics to that observed for entangled linear PEO solutions.

Introduction

Capillary gel electrophoresis is the method of choice for analyzing DNA. Historically, chemically cross-linked gels were used as sieving matrices in a slab gel format. With the introduction of capillary electrophoresis, replaceable matrices gained interest. Typically, solutions of entangled polymers are used in capillaries to sieve DNA, and since its introduction for DNA sequencing, linear polyacrylamide (LPA) has become one of the most widely used replaceable sieving matrices.[1] Since the "pores" of an entangled solution have a limited lifetime, the molecular weight window of DNA sizes that can migrate through the polymer solution is greatly increased compared to covalently cross-linked systems. Later, it was found that polymer solutions could serve as sieving media even below their entanglement threshold concentration.[2] However, the separation of small double-stranded DNA was found to be superior when using entangled polymer solutions compared to dilute unentangled solutions.[3]

The mechanisms by which polyelectrolytes migrate through a polymer matrix depend strongly on the properties of the gel.[4] Short DNA, with radius of gyration much smaller than the gel pore size, are believed to proceed by the so-called Ogston sieving mechanism. This mechanism regards the DNA molecules as rigid objects that migrate through a geometrically constrained sieve. According to this mechanism, the mobility, μ, of a spherical particle of radius R, is given by[5]

$$\ln \frac{\mu}{\mu_0} = -K_r c \quad \text{and} \quad K_r \sim (r+R)^2 \quad \text{for fiber obstacles of radius } r \tag{1}$$

where μ_0 is the free solution mobility, c the gel concentration, and K_r is the retardation coefficient. Thus, the Ogston model predicts a linear dependence between log μ and $(R_{g,DNA})^2$ when the radius of the gel fibers is much smaller than the radius of gyration of DNA ($r \ll R_{g,DNA}$).

The free-volume model gives a similar result to the Ogston model, provided that the retardation coefficient is identified with the type of obstacles that build up the gel. Namely, $K_r \sim (r + R)$ for sheetlike obstacles, $K_r \sim (r + R)^2$ for fiber obstacles, and $K_r \sim (r + R)^3$ for spherical obstacles. For these models, optimal separation is expected for DNA sizes comparable with the pore size of the gel. The Ogston model is not valid for larger DNA sizes that must alter their conformation in order to pass through the polymer network.

Larger DNA fragments travel through a matrix as a flexible chain that reptates "snakelike" through a tube.[6] This model was very successful at describing DNA sieving in entangled polymer solutions over a significant range of DNA sizes. The reptation model predicts an electrophoretic mobility that is inversely proportional to the DNA size:

$$\mu = \frac{\mu_0}{3N} \tag{2}$$

However, the experimental observation that large DNA fragments migrate with a mobility that becomes less and less dependent on DNA size led to a modification of the reptation model, namely the biased reptation model (BRM).[7−9] The assumption of this model was that very long DNA fragments in high electric fields no longer migrate as random coils. Instead they orient in the direction of the electric field, migrating in a more stretched conformation. The mobility of DNA for this case is given by

$$\frac{\mu}{\mu_0} \approx \frac{1}{3}\left(\frac{1}{N} + \frac{\epsilon_0}{3}\right) \tag{3}$$

where ϵ_0 is the electric field scaled per Kuhn length. As can be seen from this equation, the applied electric field becomes dominant for very large DNA fragments and resolution is lost.

* Corresponding author. Telephone: 626 395 4138. Fax: 626 568 8743. E-mail: jak@cheme.caltech.edu.

10.1021/ma0258253 CCC: $25.00
Published on Web 11/07/2003

So-called pluronics, triblock copolymers consisting of hydrophobic midblocks flanked by hydrophilic ones (PEO−PPO−PEO), have been studied for replaceable polymer sieving solutions. Relatively high polymer concentrations (~20 wt %) were employed that form gels consisting of micelles that packed into an fcc structure.[10,11] The mechanism of transport through these gels appears to be fundamentally different from that through random, interconnected polymer networks or entangled solutions.[12] The pluronics were found to provide high performance separations of a wide range of molecules, including oligonucleotides, double-stranded DNA fragments, and supercoiled plasmid DNAs. This was attributed to the three distinct separation domains present within the gel (hydrophobic, densely packed brushes, and less congested interbrush regions).[13]

Telechelic self-associating polymers, consisting of hydrophilic midblocks with hydrophobic ends, have also been considered for applicable sieving matrices in DNA electrophoresis. In particular, the findings regarding hydrophobically end-capped poly(ethylene glycols) are interesting for comparison with the results described in this paper. PEG polymers with fluorocarbon end groups were introduced as an effective DNA sieving media by Menchen and Winnik in 1996.[14,15] It was demonstrated that single-stranded DNA could be successfully sequenced by a mixture of C_6F_{13}- and C_8F_{17}-terminated PEGs, with a single base resolution of 440 bases. PEGs with hydrocarbon ends were shown to resolve oligonucleotides as well.[16] Above concentrations of approximately 4%, micelles of these polymers pack into a local cubic order having a mesh-size ranging from 10 to 20 nm and were found to successfully separate oligonucleotides ranging in size from 25 to 60 bases. Furthermore, it was noted that neither the Ogston nor the reptation model could describe the size-dependent mobility correctly. The most recent study involved triblock copolymers, consisting of polyoxybutylene-polyoxyethylene-polyoxybutylene (BEB).[17] Although no ordered structures were observed within these gels, very good resolution was achieved for double-stranded (ds-DNA) fragments. Relative to the pluronics, these gels provided improved resolution especially for small ds-DNA fragments. Also, the migration time was much shorter in the BEB triblock gels compared to the pluronics gels, due to the lower polymer concentration that could be used.

This paper describes the study of fluorocarbon end-capped poly(ethylene glycol)s (R_f−PEGs) as sieving media for DNA electrophoresis with an emphasis on relating the network structure to the sieving mechanisms. Fragments of double-stranded DNA were employed to study their size-dependent mobility through the self-assembling hydrogel. Issues concerning resolution are not addressed here; however, the reader is referred to earlier reports using similar hydrogel systems (fluorocarbon end-capped PEGs) to separate single-stranded DNA, where resolution is of particular importance.[14,15] Hydrophobically end-capped PEGs display a beautiful, simple linear viscoelastic behavior with a single relaxation time that depends exponentially on the hydrophobe length and only modestly on concentration. Here special attention is given to the relationship between their network topography and sieving characteristics.

Table 1. Characteristics of R_f−PEGs Used in This Study

R_f−PEG	PEG molar mass (Da)	hydrophobic end group	estimated aggregation no.[a]	micelle radius[b] (nm)
35KC8	35 000	C_8F_{17}	30	20.4
35KC10	35 000	$C_{10}F_{21}$	50	22.6
20KC8	20 000	C_8F_{17}	30	14.6
10KC8	10 000	C_8F_{17}	30	9.6
5KmPC8	5000	C_8F_{17} monosubstituted	30	9.6

[a] The aggregation number is dominated by the end group length.[29] [b] According to the Li and Witten theory.[27]

Experimental Section

Synthesis. Poly(ethylene glycols) (PEGs) with molar masses of 10 000, 20 000, and 35 000 g/mol (Fluka) were used to prepare telechelic R_f−PEGs. The synthesis was performed according to a previously published method.[18] Fluorocarbon alcohols ($C_nF_{2n+1}C_2H_4OH$, Lancaster) were reacted with an excess of difunctional linker, isophorone diisocyanate (IPDI, Aldrich) to form fluorocarbon isocyanates. The excess of IPDI was removed by vacuum distillation and several recrystallizations in hexane at −20 °C. The fluorocarbon isocyanates were then reacted in excess with the desired PEG, using dibutyltin laurate as a catalyst. The products were precipitated into cold diethyl ether and recrystallized three times from ethyl acetate. Monofunctional R_f−PEG was synthesized by a similar method, using monomethoxy PEG (with a methoxy-terminating group on one end and a hydroxy on the other end). The degree of substitution could be analyzed accurately by HPLC. Conditions for the separation were as follows: C18 column, linear solvent gradient from 70/30 H_2O/acetonitrile to 0/100 H_2O/acetonitrile in 70 min, flow rate of 0.7 mL/min, and detection by evaporative mass detector. Alternatively, the degree of end group substitution was determined by ^{19}F NMR (Delta 400 MHz) in MeOH-d_4 using sodium trifluoromethanesulfonate (Aldrich) as an internal standard (comparison was made between the CF_3 at −82.8 (hydrophobe end group) and the CF_3 at −80.6 (standard)). Characterisics of R_f−PEGs used in this study are given in Table 1.

Gels were formed by dispensing the desired amount of R_f−PEG in buffer (1xTBE). The vials with the solutions were placed in a wrist-action shaker until the gel became clear and homogeneous (1 to several days). For preparing gel mixtures, the corresponding R_f−PEGs were first dissolved in a small amount of methanol in order to obtain a fully mixed solution. Then the methanol was evaporated off and the desired amount of buffer added to the dried polymer mixture.

Rheology. A stress controlled rheometer (SR5000, Rheometric Scientific) equipped with a solvent trap was used with a cone−plate geometry (0.1 rad cone angle, 25 mm plate diameter) to obtain rheological data. Frequency sweeps were measured from 0.01 to 100 rad/s under constant stress conditions. Depending on the viscoelasticity of the sample, a stress was chosen in the range of 1−20 Pa to obtain a linear dynamic viscoelasticity.

Capillary Electrophoresis. Silica capillaries were covalently coated with either a PEG−silane (2-[methoxy(polyethyleneoxy)propyl]trimethoxysilane, Gelest) or a perfluoroalkylsilane (trichloro(*1H,1H,2H,2H*-perfluorooctyl)silane, Aldrich). Coated silica capillaries with inner diameters of 50 μm were cut in 60 cm length and a detection window was made at 36 cm from the injection side by removing the polyimide outer coating with a flame. The capillaries were connected to a 100 μL syringe (Hamilton) by PEEK fittings (Upchurch Scientific). A syringe pump system (Bioanalytical Systems) was then used to pump the gel into the capillary.

Electrophoresis experiments were performed with a home-built instrument. In brief, a high voltage power supply (CZE2000, Spellman) provided the separation and injection voltage through platinum electrodes. A laser-induced fluorescence detection setup was built for detecting the labeled DNA. A green HeNe laser (1.5 mW, 543 nm, Uniphase) was used

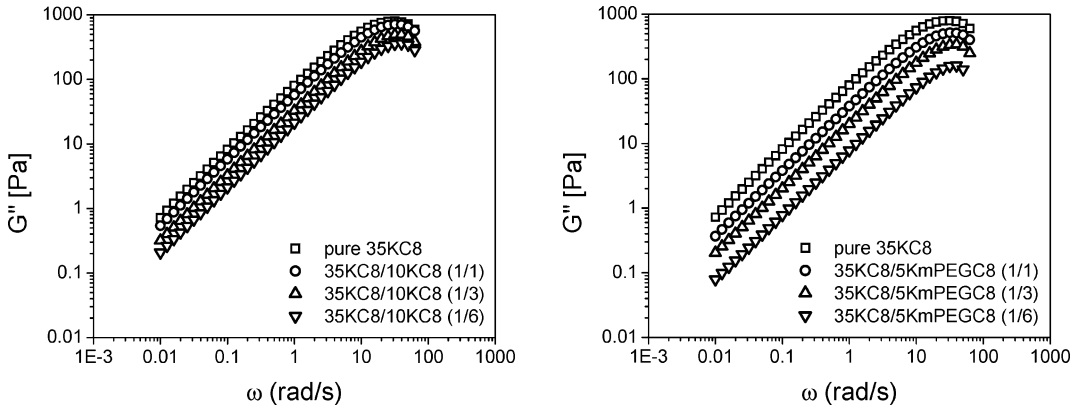

Figure 1. *G″* frequency sweeps for 35KC8 and mixtures with 10KC8 (left) and 5KmPC8 (right) all at 3.0 wt %.

for excitation. A dichroic mirror (565DCLP, Chroma) reflected the excitation light through the objective lens (M40×, Newport) on the capillary. The emitted light was collected through the same objective and further filtered by two long pass filters (Coherent COWL 560 and Edmund OG 590) and an iris (zero-aperture, Edmund Industrial Optics). A photomultiplier tube (R928, Hamamatsu) was used to measure the signal. Both the voltage supply and the photomultiplier tube were controlled and monitored by a data acquisition card (PCI 6035-E, National Instruments), using LabView software.

Gel-filled capillaries were assembled onto the holder and both cathode and anode reservoirs were filled with 1xTBE buffer. A 5 min prerun was used to stabilize the current. DNA samples were obtained from Applied Biosystems. Both DNA ladders consisted of TAMRA (tetramethyl rhodamine) labeled dsDNA fragments, ranging in sizes of 35−500 base pairs (Genescan-500) and 50−5000 base pairs (Genescan-2500). Injections of DNA were carried out electrokinetically using 133 V/cm for 10 s, directly from the supplied DNA solution containers without any dilution or additions. The capillary ends and electrodes were then placed back into the reservoirs. All runs were performed using 8 kV over 60 cm of capillary (133 V/cm). Typically, the measured current for these experiments was approximately 3 μA, which resulted in no significant heating (as observed from a linear voltage−current relation up to fields above 133 V/cm).

Results and Discussion

Dynamic Viscoelasticity. Water-soluble polymers that contain hydrophobic groups at both ends form flowerlike micelles due to association of the end groups. Above certain concentrations, the hydrophilic midblocks are able to bridge between neighboring micelles. These physically cross-linked systems find industrial applications as rheology modifiers. The viscoelastic behavior of R_f−PEGs is characterized by a single relaxation time to good approximation. The process of relaxation for these networks is governed by the exit rate (reciprocal relaxation time) of a hydrophobe from a micelle core. The relaxation time is strongly dependent on the size of the hydrophobe and slightly dependent on PEG length and polymer concentration.

To fill capillaries and microchannels with self-assembling solutions, their rheological behavior is of extreme importance. Mixing different R_f−PEGs appears to be an effective and convenient method for tuning network properties and thereby altering sieving characteristics.

At the same polymer concentration (3.0 wt %), 10KC8 forms a network that has more micelles per unit volume than 35KC8. Therefore, the average intermicelle distance is smaller for 10KC8, leading to a higher modulus for 10KC8 than 35KC8 at fixed concentration. Naively, this would lead one to expect an increase in modulus upon addition of 10KC8 to 35KC8 at fixed concentration. However, as more 10KC8 is included in the gel relative to 35KC8 the magnitude of the loss peak *decreases* (Figure 1, left). Similarly, the zero shear viscosities of the mixtures decrease from approximately 80 Pa s for the pure 35KC8 to 20 Pa s for the $^1/_6$ mixture of 35KC8/10KC8. This occurs without a shift in the relaxation time of the gel, which remains at the value characteristic of C8 fluoroalkyl ends.

Comparison of these mixtures to pure 10KC8 at the same concentration (3.0 wt %) is not possible, due to the fact that, at this overall concentration, 10KC8 separates into two equilibrium phases: a dilute sol and an equilibrium gel with c_{eq}, approximately 6.5 wt %.[19] Such comparisons are possible for "single phase" type associative thickeners. For example, Annable et al. found for C_{16} hydrocarbon end-capped PEGs with 35 and 10 kDa that the zero shear viscosity of the 35 kDa R−PEG was higher than that of the 10 kDa R−PEG at relatively low concentrations (<5 wt %), due to the different the concentrations above which the viscosity starts to rise rapidly.[20]

To clarify the mechanism of the counter-intuitive effect of 10KC8 on the viscoelastic properties of the 35KC8/10KC8 mixtures, it is instructive to examine mixtures of 35KC8 and 5KmPC8, a monofunctional PEG of 5 kDa with a single C_8F_{17} hydrophobe on one end only (i.e., a 10KC8 molecule cut in half). The *G″* curves for these mixtures (Figure 1) show a similar, yet slightly more pronounced decrease in modulus compared to the 35KC8/10KC8 mixtures. Again, the slope and maximum of the *G″* curves do not change, but now the zero shear viscosity decreases from 80 Pa s for pure 35KC8 to 7.5 Pa s for the $^1/_6$ mixture.

Given the constant aggregation number of the C8 hydrophobes (~30 R_f groups in each hydrophobic core), at fixed weight concentration (here 3.0 wt %) the number of micelles increases as shorter 10KC8 or 5KmPC8 is added to 35KC8. If the comparison were made with concentration adjusted to keep the number of micelles constant, the observed decrease in modulus with addition of 10KC8 or 5KmPC8 would be even stronger.

Clearly the similarity between the effects of adding 5KmPC8 and 10KC8 indicates that the reduction in modulus upon blending 10KC8 with 35KC8 is due to a reduction in the number of elastically effective chains upon adding the shorter R_f−PEGs to the gel. This implies that the shorter chains (i.e., the 10 kDa) predominantly form loop configurations, whereas the

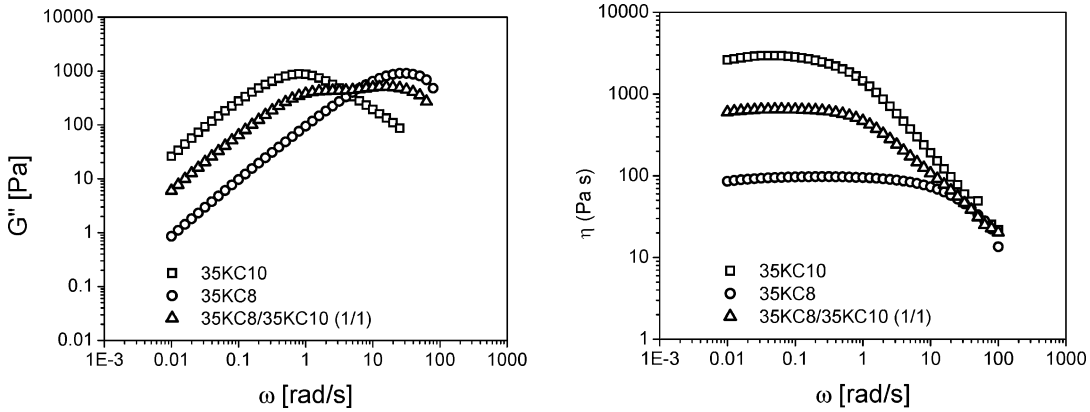

Figure 2. *G″* (left) and viscosity (right) frequency sweeps for 35KC8, 35KC10, and their mixture (all at 3.0 wt %).

longer chains (i.e., the 35 kDa) do most of the bridging. The 10 kDa chains can mainly bridge when the core-to-core distances are small enough, since they suffer too great an entropic penalty when they span a core-to-core distance substantially greater than the radius of gyration of a 10 kDa PEG. However, there must be some bridging by the shorter chains as well, to account for the milder decrease in the modulus for the 35KC8/10KC8 blends compared to the single ended short chain 35KC8/5KmPEGC8 blends. In additon to the reduction in bridging, the drop in modulus may also reflect decreased micelle−micelle repulsion. The corona immediately surrounding the micelle core is more dense, and a less dense region exists above the 5 kDa strands or 10 kDa loops; this changes the shape of the intermicelle potential in a way that makes the repulsion softer for mild distortions. Thus, the stiffness and the internal bridge:loop ratio of the gel can be modulated by blending chains of different PEG length bearing matched fluoroalkyl hydrophobes. Since the hydrophobe length governs the relaxation time of these physical gels, these changes in network topology in the blends are produced without shifting the characteristic relaxation time of the gel.

This implies that we can explore strategies to tune the distribution of relaxation times by mixing polymers that have different hydrophobe lengths. At similar concentrations the zero-shear viscosity is over an order of magnitude larger for 35KC10 compared to 35KC8 (Figure 2). This can be attributed to the slower exchange time of the $C_{10}F_{21}$ hydrophobe end groups. The *G″* curves display a similar slope and maximum value for *G″* for both 35KC8 and 35KC10. For the mixture, the *G″* curve displays a similar slope at low frequencies, followed by two apparent maxima at positions corresponding to the maxima of the pure R_f−PEGs. Therefore, both relaxation times of the two R_f−PEGs are still present in the mixed hydrogel. An important observation from a capillary gel electrophoresis point of view is that the high-frequency viscosity is independent of the hydrophobe. This means that the gels require similar pressures to be pumped into capillaries, despite the differences in their transient networks.

Capillary Gel Electrophoresis. When separating DNA in an entangled PEO solution, typically three regimes can be identified, as illustrated in Figure 3. In this example, the sieving medium consisted of a bimodal, entangled solution of 8 000 000 MW and 600 000 MW PEO. Such mixtures of linear PEO have been used before to separate DNA with high resolution.[21] The relationship between mobility, μ, and double-stranded

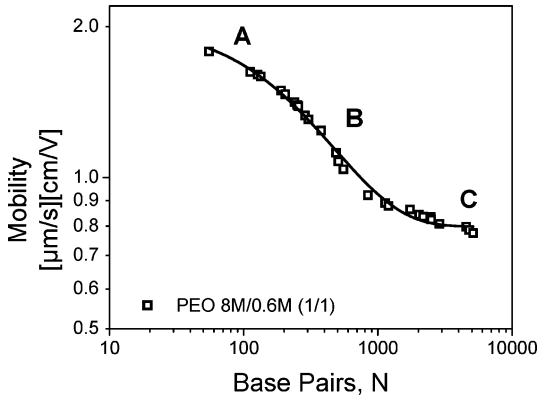

Figure 3. Mobility vs base pairs for dsDNA migration through an entangled PEO solution. The polymer matrix consists of a 1/1 mixture of PEO-8 000 000/PEO-600 000 at an overall concentration of 3.0 wt %.

DNA length, *N* base pairs, shows the typical sigmoidal shape attributed to three successive regimes: the Ogston regime (A), the reptation regime (B), and the reptation-with-orientation regime (C). The actual data could be described empirically by the following "vWBR" formula:[22]

$$\mu(N) = \frac{1}{\beta + \alpha(1 - e^{-N/\gamma})} \qquad (4)$$

where α, β, and γ are fitting parameters that have recently been related to the known gel electrophoresis theories.[23]

In contrast to previously studied PEO solutions, the present R_f−PEG hydrogels show a very different relationship between the electrophoretic mobility and DNA size. The curves are no longer sigmoidal shaped and cannot be fitted properly with the empirical vWBR formula (Figure 4).

Instead of displaying the conventional sigmoidal shape, we can identify different regimes similar to those observed by Heller.[24,25] Small fragments within zones I and II can be regarded as rigid rods. Only within zone I are the fragments small enough that they are separated by Ogston sieving, since their sizes are relatively small compared to the network mesh sizes, as discussed quantitatively below. Medium sized DNA fragments, from 400 to 1000 base pairs, are separated by reptation without orientation (zone III). The dimensions of such fragments are too large to travel as an undeformed molecule through the network. Instead, the DNA has to continuously change its conformation and move

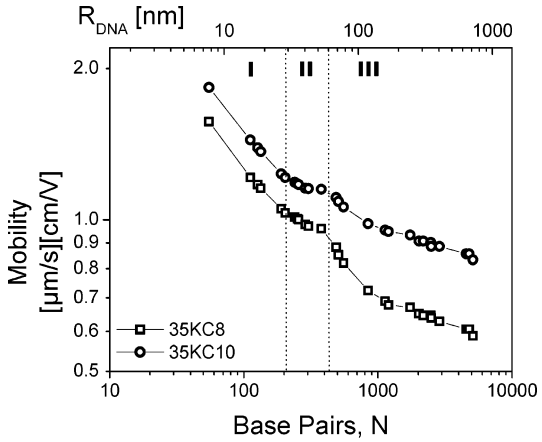

Figure 4. Mobility vs base pairs for two R_f−PEG gels, at 3.0 wt %, consisting of the same PEG length (35 kDa) but having different hydrophobe lengths (C8F17 and C10F21, respectively, for 35KC8 and 35KC10). The length of DNA (upper *x* axis) was estimated assuming a rigid rod conformation and is therefore only applicable within zones I and II.

snakelike (reptate) through the network. Larger fragments become less resolved, indicating reptation with orientation, but the transition to this zone (IV) is not complete, perhaps due to the relatively low electric field strengths used (133 V/cm) throughout this study, such that orientation may not be significant. Zone II is characterized by an approximately size-independent mobility (i.e., fragments are hardly separated). According to Heller, this regime corresponds to a situation where the DNA is larger than the gel pores, so sieving is not possible, but the DNA is still too stiff to reptate. Furthermore, Heller found that this plateau became more pronounced for higher concentrations of entangled gels, whereas in more dilute solutions, this plateau is barely visible and there is a direct transition from zone I to zone III.

This distinctive three-regime curve is found for both 35KC8 and 35KC10. Interestingly, at fixed concentration of 3.0 wt %, the overall mobility of DNA through the 35KC10 gel is *higher* compared to the 35KC8 gel. Note that this is counterintuitive based on the relaxation times of the R_f−PEGs (the fluoroalkyl ends exchange time is 40-fold slower for C10 than for C8). The reason that the end group exchange time does not control the migration velocity can be seen by considering how quickly the DNA fragments move a distance comparable to the micelle−micelle spacing. The migration velocity of the slowest, i.e., the largest, DNA fragments is still approximately 80 μm/s. On the time scale of a single relaxation of a C8 hydrophobe (∼0.03 s), such a DNA fragment travels about 2.4 μm, which corresponds to passing approximately 100 micelles. Therefore, the DNA "senses" a fixed network, even for the shorter hydrophobe length. One plausible explanation for the greater mobilities in 35KC10 than in 35KC8 is the higher aggregation number of the C10 end groups (∼50 R_f's per C10 hydrophobic core, compared to ∼30 for C8). Therefore, at fixed weight concentration, 35KC10 forms fewer micelles than 35KC8, resulting in a somewhat more open network (greater micelle−micelle distance).

To envision the physical basis for the three observed regimes of migration behavior, we provide an estimate for the DNA radius of gyration R_{DNA} (Figure 4 top), applying the Kratky−Porod formula appropriate for stiff duplex DNA (i.e., when the total curvilinear length of

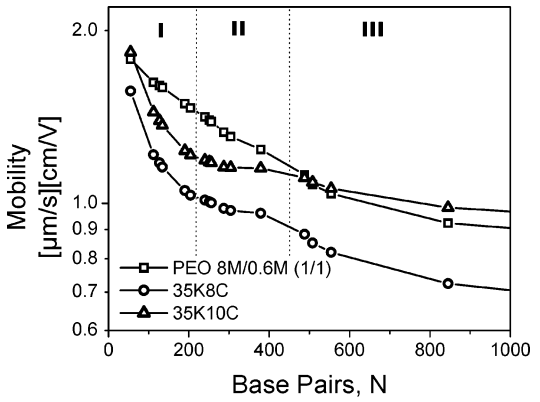

Figure 5. Ogston plot comparing the entangled polymer gel with two self-assembling R_f−PEGs (all at 3.0 wt %).

the DNA *L* is smaller than the DNA Kuhn length *b*, typically 100 nm). This assumption holds within zones I and II, and DNA can be approximated as a rigid rod:

$$\langle R_{DNA}^2 \rangle \cong \frac{1}{6} b^2 N_k^2 \tag{5}$$

where *b* is the DNA Kuhn length (∼100 nm) and N_k is the total number of Kuhn segments, given by $N_k = L/b$. Since the length of a base pair (L/N) is approximately 0.34 nm in typical electrophoresis buffers, this results in

$$\sqrt{\langle R_{DNA}^2 \rangle} \cong 0.14N \tag{6}$$

for $L < b$, which means up to approximately 300 base pairs. Therefore, this relation is appropriate in zones I and II. Note that the estimated radii shown for regime III actually overestimate the DNA size, since flexibility becomes significant.

The smallest fragments are believed to be separated according to an Ogston-sieving mechanism only within zone I. Their size is small enough (<30 nm), so they can travel undeformed through the network. Sieving proceeds by a purely free volume mechanism. So within zone I (up to ∼200 base pairs for 35KC8 and 35KC10), the so-called Ogston-plot (a semilogarithmic mobility vs base pair *N*) is expected to be linear with a negative slope. The slopes observed for both self-assembling hydrogels are much greater than found for typical entangled polymer solutions (Figure 5). Such high slopes in the Ogston-regime are typically associated with highly concentrated entangled gels or densely cross-linked networks. Here, however, it is observed for self-assembling gels at reasonably low concentration (∼3.0 wt %). The advantage of such behavior is clearly that small fragments can be separated with high resolution without the need for concentrated gels, enabling resolution with shorter capillaries and shorter run times.

Since our self-assembling network consists of interconnected flowerlike micelles, the Ogston sieving may occur through a network of spherical obstacles, rather than fiberlike ones. In that case the logarithmic mobility should scale inversely with $(r + R_{DNA})^3$, where *r* is the micelle radius. Qualitatively, this may give insight into the unusually strong dependence of mobility on DNA size that is found in these self-assembled gels (Figures 4 and 5). However, the predicted strong decrease in mobility with increasing obstacle size (micelle radius *r*) runs contrary to the higher mobility of DNA through

35KC10 than through 35KC8 (Figure 4). We now offer a physical explanation of the interesting sieving characteristics of these gels based on the structure of their self-assembled network.

We build on Heller's concept that within zone I the small DNA fragments are separated by an Ogston sieving mechanism, and that the plateau of zone II is due to the fact that the DNA fragments are too large to be sieved, but too small to reptate through the network. Therefore, we examine the regimes of sieving behavior of our gels by comparing the network "pore size" to the DNA fragment size. The present R_f−PEG networks consist of associating micelles in which the ability of telechelic chains to form bridges between micelle cores generates an entropic attraction.[26]

We can visualize the medium through which the dsDNA migrates by estimating the sizes of the micelles and the average distance between them. Li and Witten[27] described the case of a polymer brush of height R grafted on a highly curved surface (e.g., a star polymer or a micelle). A free energy minimization that balances the elastic energy from the stretching of the polymers and the excluded-volume interaction between polymers leads to a micelle radius given by

$$R = 0.914343(fN^3l^2v)^{1/5} \tag{7}$$

where f is the number of grafts (or aggregation number), N is the number of segments in a chain, and l is the segment length and v is related to the excluded volume v/l^3. This model proved to be successful at predicting micelle radii for R−PEGs consisting of 35 kDa PEG chains end-capped with C_{16} and C_{18} alkane hydrophobes.[28] Although the hydrophobe influences the aggregation number, it does not significantly alter the PEG chain dimension. We can therefore use the same relation and values for N, l, and v together with the aggregation number found for the corresponding fluorocarbon end group[18,29] and obtain an estimate of the micelle size. Furthermore, for the present materials the aggregation number has been shown to be determined by the hydrophobe only (∼50 R_f's for a C10 hydrophobic core, and ∼30 for C8). For 35KC8 a hydrodynamic radius of 25.6 nm was obtained by PGSE NMR.[18] Estimating the thermodynamic radius R and the hydrodynamic radius R_H as recommended by Russel and co-workers,[28] we obtain for 35KC8 a thermodynamic radius of 20.4 nm and a hydrodynamic radius of 15.4 nm, based on the aggregation number of 30 (R_f per hydrophobic core or $p = 15$ polymers per micelle). For the higher aggregation number for C10 fluorocarbon end groups of 50 ($p = 25$), a thermodynamic radius of 22.6 nm and a hydrodynamic radius of 18.6 nm are estimated from the model. The discrepancy between the theoretical estimate of $R_H \sim 15.4$ nm and the experimental value of 25.6 nm for 35KC8 may be due to the semiquantitative nature of the model.

The average intermicelle distance (the distance between two hydrophobic cores) for a given concentration is approximately as follows:

$$\langle d \rangle = \sqrt[3]{\frac{Mp}{cN_A}} \tag{8}$$

where M is the R_f−PEG molar mass, p is the average number of polymers per micelle (half the aggregation number), c is the gel concentration, and N_A is Avogadro's number. For 3.0 wt % gels, this results in an average distance between micelles of 30.7 nm for 35KC8 ($p = 15$) and 36.5 nm for 35KC10 ($p = 25$). Using the calculated radii for the 35KC8 and 35KC10 micelles, the degree of compression given by

$$\epsilon = \frac{R - {}^1/_2\langle d \rangle}{{}^1/_3 R} \tag{9}$$

is then 0.74 for 35KC8 and 0.58 for 35KC10. So at similar concentrations the smaller micelles of 35KC8 are relatively more compressed than the micelles of 35KC10, which may explain the slower migration of DNA fragments through the 35KC8 gel compared to the 35KC10 gel.

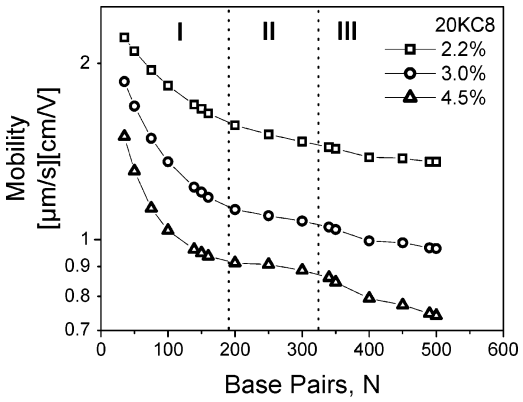

Figure 6. Mobility as a function of DNA size for different concentrations of 20KC8 gels.

It is interesting to see that the range of DNA fragments that are separated very well in zone I corresponds to sizes up to approximately 30 nm, comparable to the average distance between the micelle cores. The transition from zone I to zone II is insensitive to the hydrophobe size, consistent with the observation that the micelle radius and the distance between micelle cores are only slightly affected by the different aggregation numbers of 35KC8 and 35KC10. DNA fragments in zone II are too large to sieve through the pores in the network, yet they are too short and too stiff to reptate. In zone III, size discrimination returns, as the DNA fragments become long enough that they reptate through the network.

Effect of Gel Concentration. In accord with the observation by Heller, the plateau in zone II becomes less obvious for gels at lower concentrations (Figure 6). We believe this shift in sieving characteristics with reduced concentration arises as the "Ogston sieve" becomes more flexible, both because the micelles are less compressed against one another and because fewer of the PEG chains are in bridging configurations rather than looping back with both ends in the same hydrophobic core. Even though the average distance between micelle cores is not very sensitive to changes in concentration ($\langle d \rangle \sim c^{-1/3}$), the resulting changes in compression of the micelle coronas can be quite significant.

Although the Li and Witten model does not give quantitatively accurate results for our R_f−PEGs, we may use the model to anticipate qualitative changes in the network. Assuming similar values of the excluded volume for 20KC8 and 35KC8, the micelle radius for 20KC8 is 14.6 nm according to the Li and Witten theory. As concentration increases from 2.2% to 3.0% to 4.5%, the average distance between micelles decreases from

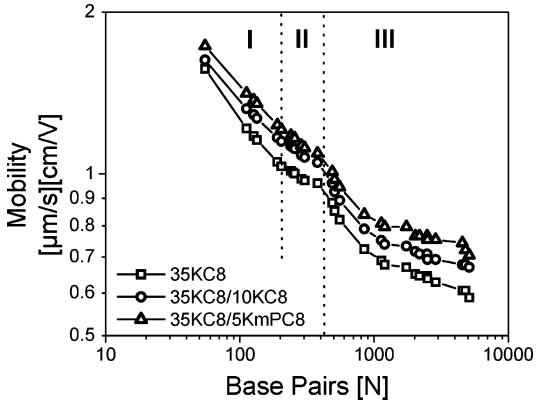

Figure 7. Mobility as a function of base pairs for a 35KC8 gel and its blends with 10KC8 and a monofunctional 5KmPC8. The concentration was 3.0 wt % for each gel.

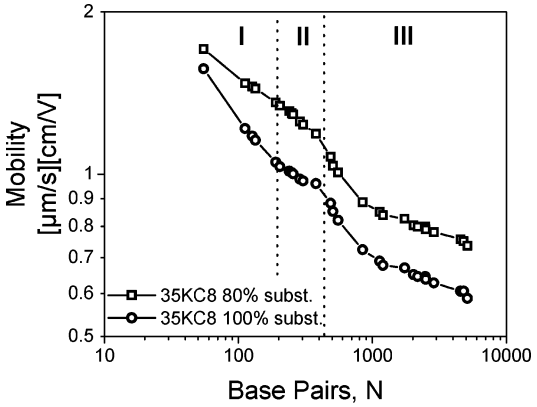

Figure 8. Mobility as a function of DNA size for two 35KC8 gels at 3.0 wt %.

28.3 to 25.5 to 22.3 nm and the degree of compression increases substantially from 0.09 to 0.38 to 0.71, respectively. In addition to the effect of the concentration on the degree of compression of micelles, it also affects the loop:bridge ratio. According to Semenov et al.[26] the number of bridges per unit area scales as

$$N_{\text{bridge}} \sim p^{5/6}\epsilon^{(2\nu+2)/(3-2\nu)} \tag{10}$$

where ν is the Flory exponent ($\nu = 0.588$), so that $N_{\text{bridge}} \sim \epsilon^{1.74}$ for relatively low degrees of compression of the micelles. The much steeper slope in zone I for the higher concentrations in Figure 6 suggests that micelle compression is important for obtaining a strong dependence of μ on N for short DNA fragments. On the other hand, the recovery of size dependence in zone II for the lowest concentration in Figure 6 suggests that reduced overlap and reduced bridging opens a distribution of passage sizes that accommodate DNA with R_{DNA} of ~30−60 nm.

Bimodal Blends of R_f—PEGs with Different PEG Lengths. The roles of micelle packing and bridging also guide interpretation of the effects on DNA sieving due to mixing R_f−PEGs with different PEG lengths. As was shown by the viscoelastic characteristics, adding shorter R_f−PEGs to longer R_f−PEG at fixed concentration alters the loop:bridge ratio. In particular, the reduction in bridging strands more than offsets the increase in number of micelles at fixed concentration, leading to a decrease in modulus and viscosity. A further consequence of the fact that shorter PEGs predominantly form loops whereas the longer PEGs account for most of the bridging is the reduced crowding of micelles near the outer corona, which may be of particular significance in facilitating migration of DNA through the gel.

In accord with the observation that adding 10KC8 to 35KC8 reduces the modulus, we also find that it shifts DNA mobilities to higher values (Figure 7), while retaining the salient features of the variations of mobility with N. Incorporation of the monofunctional R_f−PEG analogue (5KmPC8) produces a somewhat greater increase in the DNA mobility and mitigates the plateau of zone II. Again, the comparison of the effects of telechelic 10KC8 to those of monofunctional 5KmPC8 shows that the 10KC8 preferentially forms loops rather than bridges, leading to a sieving matrix that is more open than the pure 35KC8, but not quite to the extent produced by adding 5KmPC8, which cannot participate in bridging at all.

The Effect of Dangling Chains. The influence of bridging molecules also becomes very apparent when examing the effect of the degree of conversion of the end group substitution. Here we compare fully telechelic 35KC8 with a sample modified on ~80% of the PEG ends. This means that approximately 40% of the PEGs present in that sample are monofunctional, corresponding to 35KmPC8. On the basis of SANS results showing that the aggregation number per micelle core depends solely on the hydrophobe,[29] at similar concentrations and aggregation numbers, the presence of these monofunctional chains increases the distance between micelles by about 7% compared to the fully substituted R_f−PEG and significantly reduces the fraction of bridging chains. In the partially substituted sample, each hydrophobic core bears more PEG than in its fully converted counterpart, with the monofunctional PEGs particularly causing the outside corona to be less dense since it is occupied preferentially by the dangling ends. These changes in the self-assembled structure are manifested in the rheological properties of the gel: at a fixed concentration of 3.0 wt %, the zero shear viscosity of 35KC8(100%) is approximately 80 Pa s, while it is only 50 Pa s for 35KC8(80%). The effect of dangling chains on the viscoelastic properties is qualitatively similar to that observed in the 35KC8/5KmPC8 1/1 mixture containing 50 mol % 5 kDa monofunctional chains and having a zero shear viscosity of approximately 40 Pa s. (Note that both gels comprised 3.0 wt %; thus the number of micelles in the latter is greater.) These changes in network structure increase DNA mobilities and modify the separation characteristics of the gel quite significantly (Figure 8).

Within zones I and II, the change in network topology appears to alter the sieving mechanism by which the DNA is separated. The incompletely substituted R_f−PEG exhibits the desirable feature that the plateau in zone II has disappeared, with the tradeoff that the slope within zone I is less steep. This, therefore, is a strong indication that both micelle−micelle packing and bridging chains between the micelles play important roles in obtaining high-resolution separation for short dsDNA fragments. We hypothesize that the greater distance between micelle cores and the reduced bridging in the 80% substituted material are responsible for the observed changes in the resolving characteristics in zones I and II. The reduction in the concentration of hydrophobic cores in the 80% substituted case—concentration and aggregation number are fixed, so the number concentration is 20% lower in 35KC8(80%) than in

35KC8(100%)—can explain the increased mobility and reduced slope in zone I. For example, the effect of reducing the number of micelles per unit volume by changing concentration in Figure 6 showed similar effects in zone I. The increased slope in zone II for 35KC8(80%) relative to 35KC8(100%) may reflect an increased variability in the micelle−micelle network due to reduced bridging as a result of the presence of monofunctional chains. Recall that a similar increase in the slope in zone II resulted from incorporating monofunctional 5KmPC8 into 35KC8(100%) (Figure 7).

Within zone III, incomplete substitution results in higher DNA mobility, while retaining similar separation characteristics. Although the reptating DNA passes through the same concentration of polymer, the reduced connectivity and reduced micelle−micelle packing increase the mobility of the DNA. For the large DNA sizes in zone III, the migration probably occurs via a reptation-like mechanism in both 35KC8(100%) and in 35KC8(80%), explaining the similarity in the shape of the mobility vs N relationship in this zone.

Conclusions

Telechelic polymers, consisting of a hydrophilic poly(ethylene glycol) midblock, end-capped with perfluorocarbon end groups, are interesting candidates as sieving matrices for double-stranded DNA. At relatively low concentrations (>∼2 wt %) the flowerlike micelles become interconnected, building up a reversible self-assembled network. For fragments that are large enough to reptate through the network, the separation was characteristic of those observed for entangled linear polymer solutions. The topography of the interconnected micelles results in a sieving network that separates relatively small double-stranded DNA fragments with very high selectivity when the DNA fragment sizes are comparable to the distance between micelles in these gels. DNA fragments that were somewhat larger were found to have an almost size-independent mobility in monodisperse, fully telechelic gels; this regime could be changed into a size-selective one by incorporation of single-end hydrophobically modified chains. It was demonstrated that the packing and bridging between the micelles are important in determining their separation characteristics. Consequently, physical insight into the self-assembled structure of these gels can be applied to tune their sieving characteristics. One approach is to mix R_f−PEGs with different midblock lengths. Since the shorter R_f−PEGs in the mixture preferentially form loops in the network, the degree of bridging is reduced accordingly. Furthermore, by adding monofunctional substituted PEGs into the matrix, the number of bridges can be changed systematically as well. These strategies can preserve the sensitivity of mobility vs N while increasing mobility, which is advantageous for electrophoretic separation.

Acknowledgment. This research was supported in part by NSF (CTS-9729443 and MRSEC DMR-0080065), a postdoctoral fellowship from The Netherlands Organization for Scientific Research, NWO (R.G.H.L.) and by the W. M. Keck Foundation Fund for Discovery in Basic Medical Research at the California Institute of Technology. We thank Prof. Frank Gomez at the California State University of Los Angeles for helpful discussions.

References and Notes

(1) Ruiz-Matrinez, M. C.; Berka, J.; Belenkii, A.; Foret, F.; Miller, A. W.; Karger, B. L. *Anal. Chem*. **1993**, *65*, 2851.
(2) Barron, A. E.; Soane, D. S.; Blanch, H. W. *J. Chromatogr.* **1993**, *652*, 3.
(3) Mitnik, L.; Salomé, L.; Viovy, J. L.; Heller, C. *J. Chromatogr. A* **1995**, *710*, 309.
(4) Viovy, J.-L. *Rev. Mod. Phys.* **2000**, *72*, 813.
(5) Ogston, A. G. *Trans. Faraday Soc.* **1958**, *54*, 1754.
(6) Lerman, L. S.; Frisch, H. L. *Biopolymers* **1982**, *21*, 995.
(7) Lumpkin, O. J.; Dejardin, P. Zimm, B. H. *Biopolymers* **1985**, *24*, 1573.
(8) Slater, G. W.; Noolandi, J. *Phys. Rev. Lett.* **1985**, *55*, 1579.
(9) Slater, G. W.; Noolandi, J.; Turmel, C.; Lalande, M. *Biopolymers* **1988**, *27*, 509.
(10) Wu, C.; Liu, T.; Chu, B.; Scneider, D. K.; Graziano, V. *Macromolecules* **1997**, *30*, 4574.
(11) Wu, C.; Liu, T.; Chu, B. *Electrophoresis* **1998**, *19*, 231.
(12) Rill, R. L.; Locke, B. R.; Liu, Y.; Van Winkle, D. H. *Proc. Natl. Acad. Sci. U.S.A.* **1998**, *95*, 1534.
(13) Rill, R. L.; Liu, Y.; Ramey, B. A.; Van Winkle, D. H.; Locke, B. R. *Chromatogr. Suppl. I* **1999**, *49*, S-65.
(14) Menchen, S.; Johnson, B.; Winnik, M. A.; Xu, B. *Chem. Mater.* **1996**, *8*, 2205.
(15) Menchen, S.; Johnson, B.; Winnik, M. A.; Xu, B. *Electrophoresis* **1996**, *17*, 1451.
(16) Magnusdottir, S.; Viovy, J.-L.; François, J. *Electrophoresis* **1998**, *19*, 1699.
(17) Liu, T.; Liang, D.; Song, L.; Nace, V. M.; Chu, B. *Electrophoresis* **2001**, *22*, 449.
(18) Xu, B.; Li, L.; Yekta, A.; Masoumi, Z.; Kanagalingam, S.; Winnik, M. A.; Zhang, K.; Macdonald, P.; Menchen, S. *Langmuir* **1997**, *13*, 2447.
(19) Tae, G.; Kornfield, J. A.; Hubbell, J. A.; Johannsmann, D.; Hogen-Esch, T. E. *Macromolecules* **2001**, *34*, 6409.
(20) Annable, T.; Buscall, R.; Ettelaie, R. *J. Rheol.* **1993**, *37*, 695.
(21) Kim, Y.; Yeung, E. S. *J. Chromatogr. A* **1997**, *781*, 315.
(22) Van Winkle, D. H.; Beheshti, A.; Rill, R. L. *Electrophoresis* **2002**, *23*, 15.
(23) Slater, G. W. *Electrophoresis* **2002**, *23*, 1410.
(24) Heller, C. *Electrophoresis* **1999**, *20*, 1962.
(25) Heller, C. *Electrophoresis* **2001**, *22*, 629.
(26) Semenov, A. N.; Joanny, J.-F.; Khokhlov, A. R. *Macromolecules* **1995**, *28*, 1066.
(27) Li, H.; Witten, T. A. *Macromolecules* **1994**, *27*, 449.
(28) Pham, Q. T.; Russel, W. B.; Thibeault, J. C.; Lau, W. *Macromolecules* **1999**, *32*, 2996.
(29) Tae, G.; Kornfield, J. A.; Hubbell, J.; Lal, J. *Macromolecules* **2002**, *35*, 4448.

MA0258253